THE SUPERHEATING FIELD OF NIOBIUM: THEORY AND EXPERIMENT

N. Valles† and M. Liepe, Cornell University, CLASSE, Ithaca, NY 14853, USA

Abstract

This study discusses the superheating field of Niobium, a metastable state, which sets the upper limit of sustainable magnetic fields on the surface of a superconductors before flux starts to penetrate into the material. Current models for the superheating field are discussed, and experimental results are presented for niobium obtained through pulsed, high power measurements performed at Cornell. Material preparation is also shown to be an important parameter in exploring other regions of the superheating field, and fundamental limits are presented based upon these experimental and theoretical results.

INTRODUCTION

An important property of superconductors that has posed both theoretical and experimental challenges is the magnetic superheating field, a metastable state wherein the material remains fully superconducting above the respective critical fields in steady state. Obtaining accurate measurements of this metastable state is essential to expand the theoretical understanding of this phenomena and determine the ultimate limit of radio-frequency superconductors. In this study, niobium is used to probe this limiting field.

Studying the superheating field is important on several counts. First, current theoretical models can immediately be tested against measurements. Second, the regions in which empirical methods accurately describe the field tend to be in limiting cases, such as the low- or high-κ limit,[1, 2] or in small temperature ranges around the critical temperature.[3] Measuring the superheating field in the intermediate range, where $\kappa \sim 1$, provides an important result that can guide development of new models covering the entire range of κ. Third, most models are based upon a phenomenological model of the superheating field, only valid near T_c, and so say nothing about the behaviour as a function of temperature. Newer, non-phenomenological calculations taking temperature dependence into account need accurate data to test against. Finally, the accurate determination of the superheating field also is of particular interest in application. While theory and experiment agree near T_c, niobium microwave cavities for particle accelerators operate at temperatures $< T_c/4$, where theory and experiment are disparate, so measurements can set stringent upper limits for what is possible with these cavities.

This paper begins with a brief review of the the critical fields of superconductors, discusses the current state of knowledge on the superheating field and then presents new research being done at Cornell to probe this phenomena. Finally, the implications of the work presented here are discussed and regions for further study are explored.

* Work supported by DOE award ER41628
† *nrv5@cornell.edu

Critical Fields of Superconductors

When a superconductor in a constant magnetic field is cooled below its critical temperature, it expels the magnetic field from the bulk of the superconductor. This is accomplished by superconducting electrons establishing a magnetization cancelling the applied field in the bulk of the material. The magnetic is field limited to a small region close to the surface, characterized by a penetration depth λ, which is the region in which supercurrents flow. Another important length scale in superconductors is the coherence length, ξ_0 which is related to the spatial variation of the superconducting electron density. The ratio of these characteristic length scales yields the Ginsburg-Landau (GL) parameter, $\kappa \equiv \lambda/\xi$.

Pippard improved upon the superconductor model that only assumed local electron interaction to take into account non-local effects. He argued that superconducting wavefunctions should have a characteristic dimension ξ_0. If only electrons around $k_B T_c$ of the Fermi energy can be involved in the dynamics around the critical temperature, and they have a momentum range $\Delta p \approx k_B T_c/v_F$, where v_F is the Fermi velocity, then the approximate coherence length should, by the uncertainty principle be

$$\Delta x \sim \frac{\hbar}{\Delta p} \quad \rightarrow \quad \xi_0 \sim \frac{\hbar v_F}{k_B T_c}. \tag{1}$$

Assuming a pure material has a coherence length ξ_0, Pippard showed that if impurities introduce scattering centers giving an electron mean free path of ℓ, then the coherence length of the impure material, ξ, is modified to be

$$\frac{1}{\xi} = \frac{1}{\xi_0} + \frac{1}{\ell}, \tag{2}$$

and the penetration depth becomes

$$\lambda = \lambda_L \sqrt{1 + \frac{\xi_0}{\ell}}, \tag{3}$$

where λ_L is the mean free-path of the material with no scattering sites.[4]

These expressions can be used to give κ as a function of mean free path:

$$\kappa(\ell) = \frac{\lambda_L}{\xi_0} \left(\frac{\xi_0 + \ell}{\ell} \right)^{3/2}. \tag{4}$$

The ratio κ separates superconductors into two broad categories; those with $\kappa < 1/\sqrt{2}$ are called Type-I superconductors and those with $\kappa > 1/\sqrt{2}$ are called Type-II superconductors. The implications of this categorization will be elaborated upon later in this paper.

The superconducting state is more ordered than the normal conducting state because of the Cooper pairing of electrons near the Fermi energy. Subjecting a material to a DC magnetic field causes supercurrents to flow in the layer within a penetration depth of the superconducting surface to cancel out interior fields, which raises the free-energy of the superconductor, F_s, which depends on the applied field. When F_s is equal to the free energy of the normal conducting state, F_n, flux enters the superconductor, of volume V_s, and a phase transition occurs.

Mathematically, one can write an expression for the critical field that causes this phase transition, H_c,

$$F_n = F_s(H=0) + \mu_0 V_s \int_0^{H_c} H \, dH, \tag{5}$$

which is applicable for Type-I superconductors in steady-state conditions.

Supposing the energy density of superconductors is suppressed over a coherence length ξ_0, the free energy per unit area would be increased by

$$\frac{\mu_0}{2} H_c^2 \xi_0. \tag{6}$$

If magnetic field, H_e is admitted to penetrate the material a distance λ, the free energy is lowered by

$$-\frac{\mu_0}{2} H_e^2 \lambda, \tag{7}$$

giving a net boundary energy per unit area of

$$\frac{\mu_0}{2}\left(\xi_0 H_c^2 - \lambda H_e^2\right) \tag{8}$$

Type-II superconductors, (having $\xi_0 < \lambda$) can benefit from a negative surface energy gain by allowing flux tubes into the bulk of a superconductor at a field H_{c1}, which by definition is below the field H_c. The superconductor is then in a mixed state having normal conducting regions interpenetrating the bulk material, up to a field H_{c2} when the entire material transitions into the normal state.

An expression relating H_{c1} and H_c, was given by Merrill[5] as

$$H_{c1} = \left(\ln\kappa + \frac{0.08}{\sqrt{2}\kappa}\right) H_c \tag{9}$$

The thermodynamic critical field and H_{c2} are related according to

$$H_c = \frac{H_{c2}}{\sqrt{2}\kappa}. \tag{10}$$

There is one more type of critical field, denoted H_{c3} that is a surface effect first predicted by Saint-James and de Gennes. Because real superconductors are finite in size, the behaviour near the surfaces must be taken into account. For fields parallel to a superconducting surface, above H_{c2} superconductivity can nucleate at a metal-insulator interfaces, though the bulk remains normal conducting.

Both theory and experiment have shown that for fields of magnitude

$$H_{c3} = 1.695 H_{c2} \tag{11}$$

a superconducting surface sheath of thickness ξ persists, while the bulk is normal conducting. This field dominates a different type of phenomena compared with the other critical fields, because of the depth dependence of the state. The other fields have constant depth profiles, either being in the Meissner state or normal conducting state, where as H_{c3} transitions from superconducting to normal as depth increases. Finally, the field orientation for the other fields is normal to the surface, whereas for H_{c3} the field is parallel to the surface.

Metastability So far, these critical fields mentioned are in equilibrium conditions. Before a transition takes place, there is an energy cost to nucleate a fluxoid, which leaves open the possibility of a metastable state in which the energetically favorable transition has not occurred due to the activation energy barrier. This barrier vanishes at the superheating field, H_{sh}.

Both Type-I and Type-II superconductors can persist in the Meissner state above H_{c1}. The precise relationship between H_{sh} and H_c is still a field of active experimental and theoretical research, but a phenomenological result shows that near T_c

$$H_{sh} = c(\kappa) H_c \left[1 - \left(\frac{T}{T_c}\right)^2\right], \tag{12}$$

where $c(\kappa)$ is the ratio of the superheating field and the thermodynamic critical field. The determination of this factor is one of the central focuses of this work.

SURVEY OF PREVIOUS WORK

Theoretical Survey

The superheating field has been studied in several regimes, mostly with phenomenological treatments through Ginzburg-Landau theory and is a challenging field to determine theoretically. Because it has been the most frequently used tools to study superconductivity, here we outline the basic tenets of the GL Model.

Ginzburg and Landau approached superconductivity phenomenologically by introducing a parameter $\kappa = \frac{\lambda}{\xi}$, that is the ratio of the two characteristic lengths in a superconductor which can be used to broadly characterize superconductors into two classes, Type-I, with $\kappa < \frac{1}{\sqrt{2}}$ and Type-II having $\frac{1}{\sqrt{2}} < \kappa$.

The basic postulate of GL theory is that if ψ, a pseudo-wavefunction that is the order parameter corresponding to the number of superconducting electrons, varies slowly in

space then the free energy density f can be expanded in a series of the form

$$f = f_{n0} + \alpha|\psi|^2 + \frac{\beta}{2}|\psi|^4 + \frac{1}{2m^*}\left|\left(\frac{\hbar}{i}\nabla - q^*\mathbf{A}\right)\psi\right|^2 + \frac{\mu_0 h^2}{2}, \quad (13)$$

where f_{n0} is the free energy of the normal conducting state, m^* and q^* are the effective particle mass and charge and h is the applied field. A derivation of the superheating field as a function of κ requires a stability analysis and is beyond the scope of this paper, so it suffices to say that this work was completed by Matricon and Saint-James, wherein they calculated that the superheating field has values shown in the phase diagram in Fig. 1.

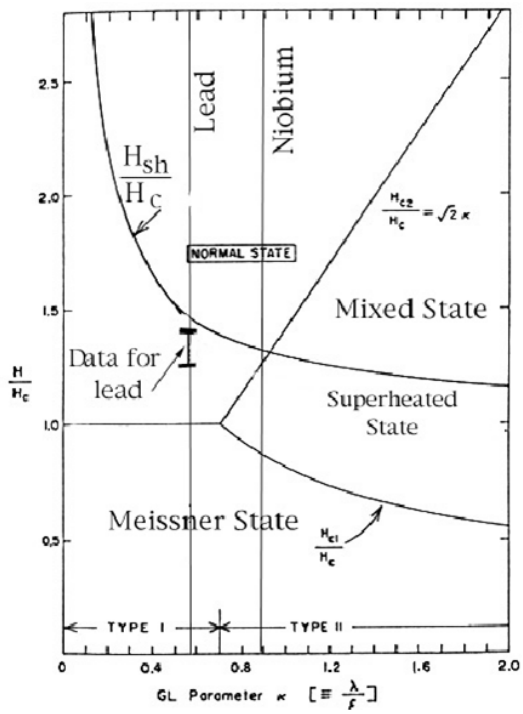

Figure 1: Phase diagram of magnetic field vs κ for superconductors in the intermediate κ range. Note that above the Meisner state for both Type-I and Type-II superconductors, a metastable superheating field exists that, in the stable state, would be either a normal conducting or mixed state. The line showing the superheating field was solved by Matricon and Saint-James[6].

The phenomenological approach gives insight into H_{sh} near T_c but to investigate its behaviour over a range of temperatures a more physically complete theory is required.

In principle BCS theory should allow a complete understanding of the superheating field. In practice, however, currently it is not known how to compute the superheating field within this context, nor even how to correctly formulate the problem. Thus, another theory is necessary to make progress on this front.

To this end, two simpler theories, the Eilenberger equations and Eliashberg theory, allow determination of the superheating field as a function of temperature. Eliashberg theory[7] requires the full information about the electronic structure of the superconductor and is very difficult to solve. The Eilenberger equations,[8] while also very challenging to solve, have been the subject of significant recent theoretical progress, and thus provide the best theoretical understanding to date.[2]

Experimental Survey

Much of the work with the superheating field has been through using the RF critical field (H_c^{RF}), or largest RF magnetic field that can be applied to a sample while it remains superconducting, as a proxy for the superheating field. The reason they are not equivalent is that the critical RF field can be limited by material defects causing superconductivity to quench at low fields. Nevertheless, for a perfect sample, one would expect that the critical RF field is limited only by H_{sh} since that is a fundamental material property.

Finnemore et. al. measured H_c, H_{c1} and H_{c2} for high purity samples of Niobium using magnetization curves, using an apparatus illustrated in Fig. 2 and noted that when measuring H_{c1}, "a final, steady-state value of the magnetization is sometimes obtained only after 10 or 20 sample translations. It is as if vibration assists the flux movement into or out of the sample."[9] Though they did not assert that the values above H_{c1} were superheating fields, it seems likely that these metastable states were evidence of superheating, and a similar set-up was used by Doll and Graf to measure the superheating in Sn samples, suggesting an apparatus based this schematic is suitable to measure superheating in Niobium.

The first measurement confirming that the superheating field of niobium is greater than the thermodynamic critical field, H_c was reported in 1967 by Renard and Rocher[10]. They used magnetization curves of very pure Nb cylinders at 4.2K to demonstrate this fact, and set the stage for subsequent measurements.

The superheating field near the critical temperature, T_c, has been measured for several Type-I materials, such as In, Sn, and Pb, as well as with a few alloys of SnIn and InBi that are Type-II[11]. A plot of the phase diagram along with several measurements of critical RF fields are presented in Fig. 3. Yogi claims that DC superheating was also seen in these samples, but it was only approximately a 10% effect. His work did not take into account the temperature variation of the superheating field, and was only done at temperatures just under T_c.

Measurements of the RF critical field were made by Campisi and Farkas at SLAC,[12, 13], and later by Hays at Cornell[14]. The results of Hay's this test are presented in Fig. 4. In all cases they found that near T_c, the data followed the GL prediction but the maximum fields achieved in the fully superconducting state were lower then the theoretical predictions for the superheating field at low temperatures.

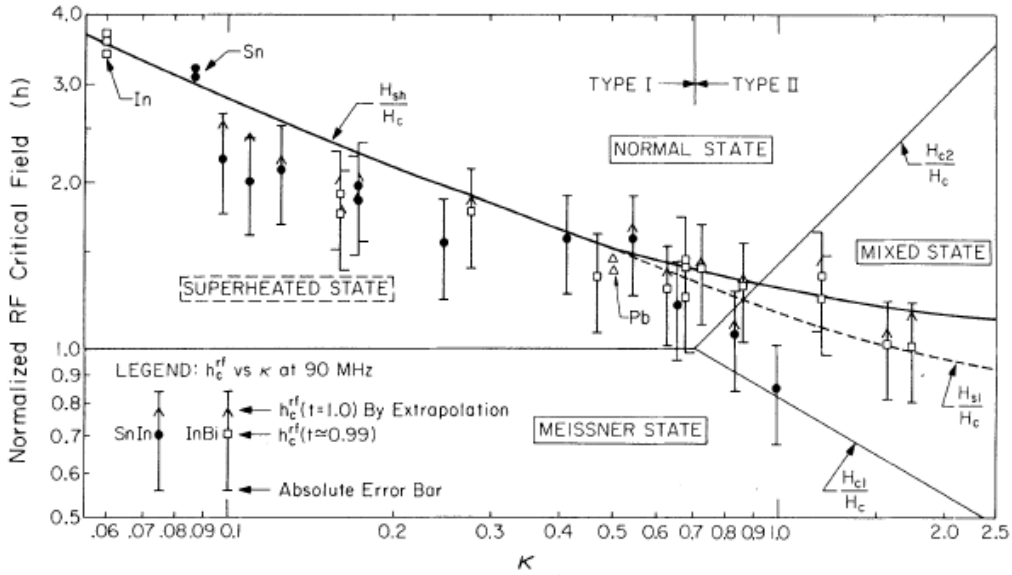

Figure 3: (Figure and caption reproduction from [11]) Normalized critical fields as a function of the Ginzburg-Landau parameter κ. Data points are for $h_c^{RF} = H_c^{RF}/H_c$ at $t = T/T_c = 0.99$ for several metals and alloys. Full curve is the calculation (Matricon and Saint-James) of the DC superheating field.

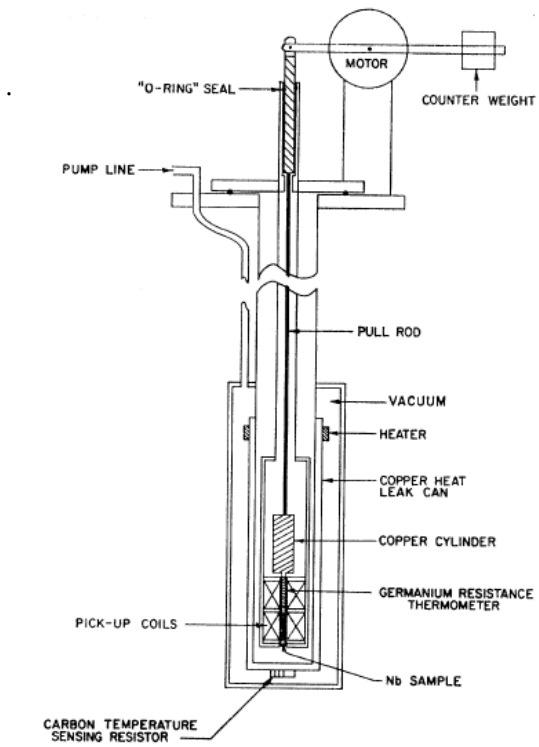

Figure 2: (Figure reproduced from [9]) Schematic of experimental setup used to measure critical fields of small, high-purity niobium samples.

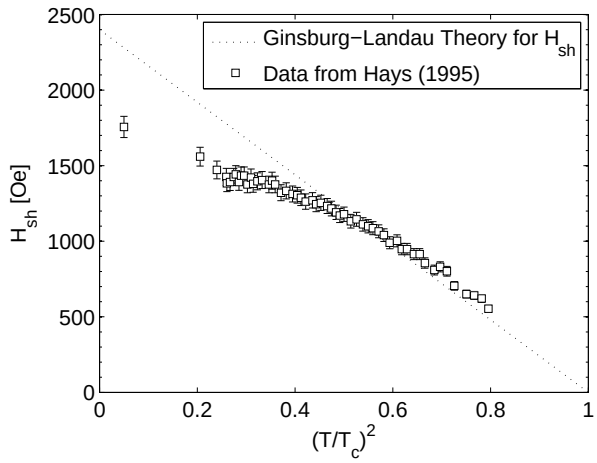

Figure 4: Measurement of the maximum surface magnetic field of niobium from Hays and Padamsee, using a 1.3 GHz cavity that received a buffered chemical polish surface treatment and did not receive a final low temperature heat treatment.[14] Ginzburg-Landau theory predicts $H_{sh} = 1.2H_c[1 - (T/T_c)^2]$ near T_c for pure niobium. At high temperatures the data agrees with theory but flattens out at low temperatures, likely due to defects causing premature flux entry or thermal heating warming up the RF surface of the cavity above the LHe bath temperature.

NEW SUPERHEATING FIELD RESULTS

In this section, we first present the theoretical results of the superheating field coefficient from the Eilenberger equations, then outline the methods used to measure the superheating fields in RF and finally present new measurements of the superheating field of Niobium.

New Theoretical Results

The constant $c(\kappa) \equiv H_{sh}(0)/H_c$ in Eq. 12 is dependent on the order parameter of the material, $\kappa = \lambda/\xi$, which is the ratio of the penetration depth and coherence length of the material. The Eilenberger equations have been solved near T_c to yield Fig. 5.[15]

Furthermore, the significant progress on the temperature dependence of the superheating field has been made for temperatures as low as $0.2T_c$, in the case of $\kappa \sim 1$ under DC conditions, and these results will soon be available to test against theory.[15]

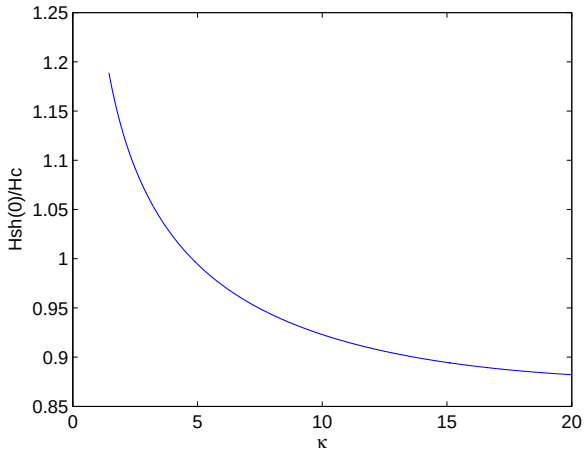

Figure 5: Plot of the ratio of the superheating field and the thermodynamic critical field, H_c, at zero temperature, versus the Ginsburg-Landau parameter, κ.[15]

RF Measurement Method

The RF superheating field of niobium can be measured by using high power pulses to drive a superconducting cavity and noting at what field level the cavity transitions from the superconducting to the normal conducting state. If the location of the quench can be determined, and is found to be global, then the limiting field is a fundamental property of the material, not simply that of a localized defect, and suggest that the superheating field was reached. By placing thermometry on the outer cavity wall one can determine the temperature dependence of the superheating field and compare it with predictions.

In practice at Cornell, the tool used to measure the superheating field would be a 1.3 GHz niobium resonating cavity driven by a klystrons capable of supplying 1.5 MW pulses with durations 50-500 μs. Short, high power pulses prevents the cavity from heating significantly as the field in the cavity ramps up, meaning that the temperature measured at the outer cavity surface is also the temperature of the inner surface. When the magnetic field on the cavity surface reaches the superheating field, H_{sh}, the niobium wall undergoes a phase transition into the normal conducting state.

By calculating the quality factor, a number proportional to how many RF cycles it takes to dissipate the energy stored in a system, during the pulse, one can pinpoint the time the cavity transitioned into the normal conducting state and what the surface magnetic fields were at this time, yielding the superheating field. How one determines the quality factor of the cavity during the pulse is addressed next.

Calculation of Q_0 as a Function of Time

To accurately measure the superheating field, it is essential to determine precisely when the cavity transitions to the normal conducting state. Previous work has shown that a niobium cavity remains at least 90% superconducting as long as the intrinsic quality factor is greater than 2×10^6.[14, 16] It has been shown how to determine the quality factor as a function of time in several publications,[13, 12, 14, 16] but the argument is reproduced here for completeness.

A cavity driven on resonance, at an angular frequency ω, by a single input coupler with an incident power, P_f, reflects some power, P_r, stores energy in the field in the cavity, U, and dissipates some energy in the cavity walls, $P_d = \frac{\omega U}{Q_0}$, where Q_0 is the quality factor of the cavity. Conservation of energy gives:

$$P_f = P_r + \frac{\omega U}{Q_0} + \frac{dU}{dt} \tag{14}$$

The reflected power is not a measured quantity, so another expression relating P_r and P_f is needed. A full derivation of the needed equation is presented in Padamsee et. al., Chap. 8;[17] in this paper only a plausibility argument will be made, and the result quoted.

The reflected power is the superposition of the reflection of the incident power signal, and the power emitted from the cavity through the coupler. The reflection coefficient of the cavity can be expressed in terms of the admittances of the waveguide and the cavity-coupler system. Expressing these admittances in terms of cavity parameters one finds

$$\sqrt{P_r} = \sqrt{P_f} - \sqrt{P_e}. \tag{15}$$

where $P_e = \frac{\omega U}{Q_{ext}}$ is the power losses through the coupler with an external quality factor of Q_{ext}.

Using P_r from Eq. 15 in Eq. 14 yields the expression

$$\frac{\omega U}{Q_0} = 2\sqrt{\frac{\omega U P_f}{Q_{ext}}} - \frac{dU}{dt} - \frac{\omega U}{Q_{ext}} \tag{16}$$

The final expression can be obtained by using the identity $\frac{d\sqrt{U}}{dt} = \frac{1}{2\sqrt{U}}\frac{dU}{dt}$ to yield

$$\frac{1}{Q_0} = \frac{2}{\omega\sqrt{U}}\left(\sqrt{\frac{\omega P_f}{Q_{ext}}} - \frac{d\sqrt{U}}{dt}\right) - \frac{1}{Q_{ext}} \tag{17}$$

Equation 17 allows one to calculate Q_0 as a function of time from measurements of P_f and U. Finding the time when the quality factor of the cavity falls bellow 2×10^6 pinpoints when the cavity transitions into the normal conducting state.[14]

An example demonstrating how this method is used to determine the critical field is presented in Fig. 6.

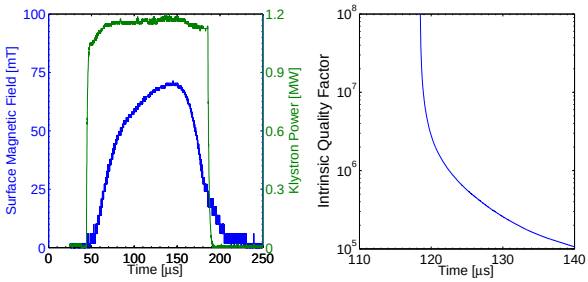

Figure 6: (Color online) Left: A trace showing the square power wave incident on the cavity (green) and the surface magnetic field of the cavity (blue) taken at 7.2 K. Right: Plot of Q_0 vs time. The actual transition into the normal conducting or mixed state can be at fields below the maximum magnetic field during a pulse, so accurately determining time of phase transition is essential. The plot shows that $Q = 2 \times 10^6$ at 120.6 μs. This corresponds to $H_{sh} = 66.4$ mT.

Test Results

A 1.3 GHz re-entrant shaped Nb cavity, LR1-3 was used to probe the superheating field. The cavity received a vertical electropolish, a two hour high pressure rise (HPR) followed by a clean assembly. Finally it was baked at 120 °C for 48 hours, a process known to mitigate the effects of high field Q-slope[18].

The cavity was first tested in continuous wave (CW) mode to measure its properties. Its intrinsic quality factor as a function of accelerating gradient is shown in Fig. 7. The cavity reached accelerating electric fields up to 42 MV/m in CW operation, corresponding to a maximum surface magnetic field of 147.4 mT, and demonstrates a strong decrease in Q_0 (i.e. increase in surface resistivity) at high fields. In spite of the degradation of the quality factor at high fields, heating losses at this level do not cause significant global heating in pulse mode cavity operation.

The quality factor was also measured as a function of temperature in CW operation. This information can be used to determine the surface resistivity of the cavity from the relation $R_s = G/Q_0$, where G is the geometry factor (283.1 Ω for the cavity tested) and Q_0 is the intrinsic quality factor. Plots of these quantities versus temperature are presented in Fig. 8.

The surface resistivity of the cavity has two contributions, a temperature independent residual resistivity, R_0,

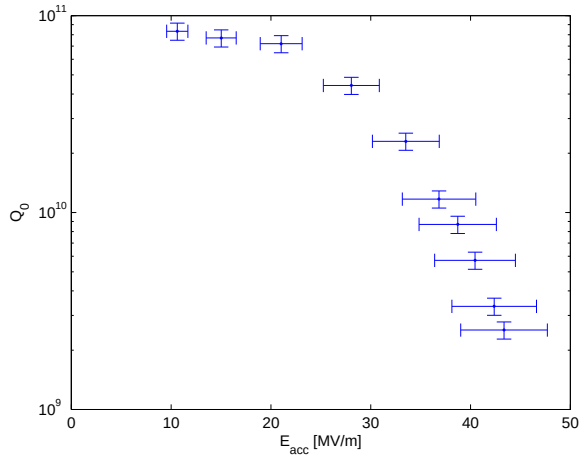

Figure 7: A continuous wave Q vs E curve taken at 1.7 K for cavity LR1-3. The Q degrades as the accelerating gradient is increased.

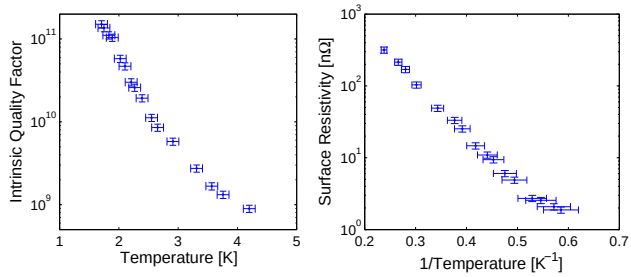

Figure 8: Left: Quality factor of the cavity as a function of temperature. The cavity had a quality factor of 1.5×10^{11} at 1.7 K. Right: The Surface resistivity of the cavity as a function of temperature. The residual resistivity of the cavity is (0.92 ± 0.23) nΩ. Data was taken at an accelerating gradient of 6 MV/m.

and the BCS surface resistivity:

$$R_s(T) = R_0 + A(f, \ell, T) \exp\left(-\frac{\Delta}{k_b T_c}\frac{T_c}{T}\right) \qquad (18)$$

where A is a function of the frequency, f, mean free path, ℓ and temperature, T. The residual resistivity of the cavity is found to be $R_0 = (0.92 \pm 0.23)$ nΩ from the low temperature data.

Subtracting the residual resistivity from the surface resistivity leaves the BCS resistivity which can be calculated from material properties. A Fortran code, SRIMP,[19] based on the Halbritter definitions, was used to fit the measured BCS surface resistivity by varying the energy gap, $\Delta(0)$ and mean free path, ℓ, of the material. The parameters used in the data fit are listed in Table 1.

The resulting fit is displayed in Fig. 9, and was fit with parameters $\Delta(0)/k_B = 18.9 \pm 0.3$ K and $\ell = (26.9 \pm 1.2)$ nm. This small mean free path is consistent with results after low temperature baking obtained by Ciovati.[20]

Table 1: Material properties used in the calculation of BCS resistivity of the niobium.

Input Parameter	Value
Frequency	1294.5 MHz
Critical Temperature	8.83 K
Coherence Length	640 Å
London Penetration Depth	360 Å
Fit Parameters	**Values**
Energy Gap $\left(\frac{\Delta(0)}{k_B}\right)$	(18.9±0.3) K
Mean Free Path	(26.9±1.2) nm

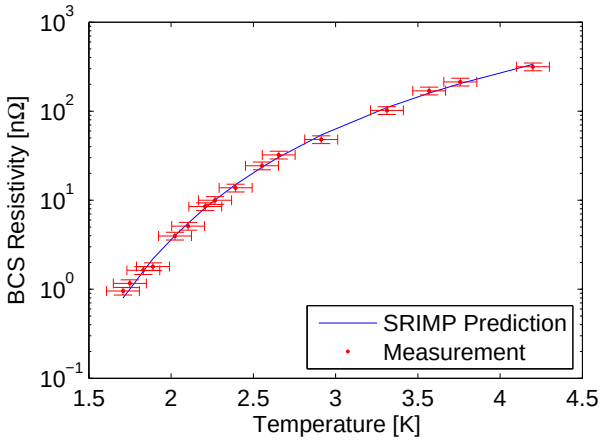

Figure 9: The BCS resistivity versus temperature. The blue line is the results of a code, SRIMP, which calculates BCS resistivity from material properties. This fit gives the mean free path estimate of $\ell = (26.9 \pm 1.2)$ nm.

From Eq. 4, the mean free path corresponds to a Ginsburg-Landau parameter $\kappa = 3.49 \pm 0.16$, showing that the decreased mean free path of the niobium causes it to become a more strongly Type-II superconductor. Referencing Figs. 5 yields $H_{sh}(0)/H_c = 1.044 \pm 0.001$, for the theoretical prediction near T_c based on the Eilenberger equations. The superheating field near T_c is then

$$H_{sh}(T) = (1.044 \pm 0.001) H_c \left[1 - \left(\frac{T}{T_c}\right)^2\right]. \quad (19)$$

The pulsed measurements of the superheating field versus normalized temperature squared are presented in Fig. 10. A linear fit was performed on the data, giving the result

$$H_{sh}(T) = \left[(197.9 \pm 5.8) - (215.1 \pm 13.0)\left(\frac{T}{T_c}\right)^2\right] \text{mT}. \quad (20)$$

For a material with $\kappa = 3.5$, the superheating field coefficient is $c(\kappa) = 1.05$, meaning that the measured results are in very good agreement with theoretical predictions.

Since the high-temperature bake is known to introduce scattering impurities into the RF layer, and thereby cause Nb to become more strongly Type-II, we sought to make

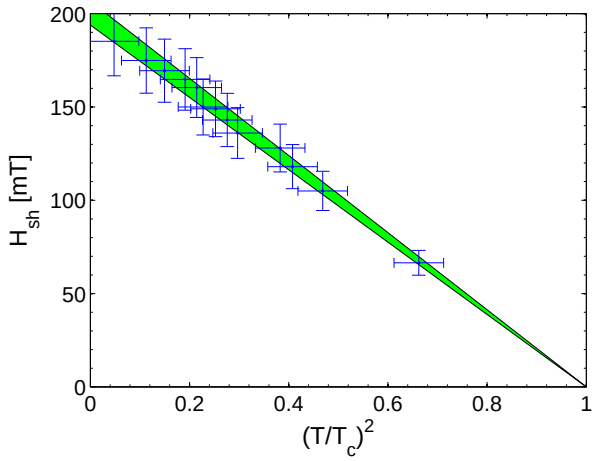

Figure 10: Measurements of the superheating field plotted versus $(T/T_c)^2$, where $T_c = 8.83$ K. The green cone is the Ginsburg-Landau prediction for niobium with a mean free path of (26.9 ± 1.2) nm, including the uncertainty in the ratio of $H_{sh}(0)/H_c$.

the same measurements for a samble with κ closer to 1. This would have the effect of increasing the superheating field coefficient in Eq. 12, from Fig. 5.

To this end, the cavity was baked at 800 °C, recieved another vertical electropolish, and was HPRed for 2 hours and cleanly assembled. To keep the electron mean free path at a large value, the cavity was not baked at 120 °C.

As before CW measurements of the quality factor were performed. A plot of the second Q vs E curve is shown in Fig. 11. In this case, the lack of low temperature bake did not suppress the high field Q-slope and the Q vs E curve shows very strong quality factor degradation above 25 MV/m, as expected for an unbaked cavity.

The results of the second set of pulsed measurements are presented in Fig. 12. Fitting the points near T_c, it is clear that the material κ has changed to $\kappa \sim 1$. The strong high field Q-slope resulted in significant heating at lower temperatures and higher fields, preventing the superheating field from being measured at low temperatures.

CONCLUSIONS

The work presented here demonstrates the first measurement of the full temperature dependence of the superheating field. The results show that while the phenomenological model is not a complete description of the superheating field mechanism at low temperatures, it is a surprisingly accurate description over the full temperature range. This suggests that the Meissner state may metastably persist to between 200–250 mT in Nb at low temperatures.

Furthermore, these results show that surfaces treated by the standard high gradient cavity preparation treatments strongly influence the superheating field. The mechanism in this study is related to the change in electron mean free

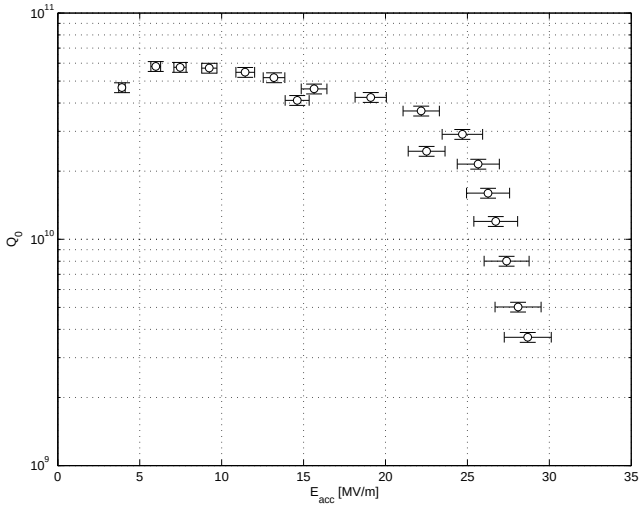

Figure 11: Quality factor versus accelerating field taken at 1.6K for LR1-3 after standard cavity processing without 120°C bake. Note the very strong high field Q-slope. The cavity did not exhibit field-emission but was power limited.

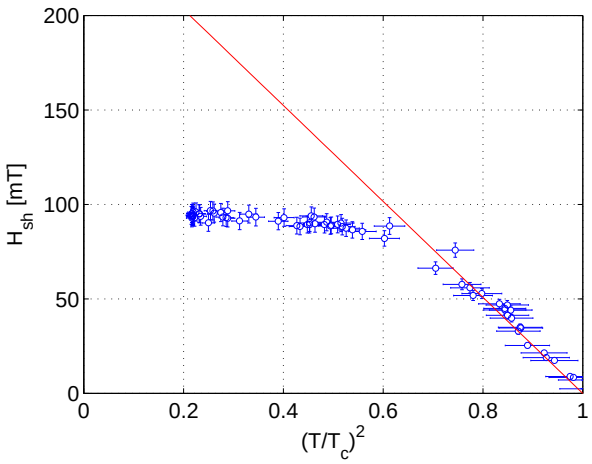

Figure 12: Superheating field measurements for the unbaked cavity. The coefficient from Eq. 12 from the data near T_c is $c(\kappa) = 1.28 \pm 0.06$. This shows that κ for the material has changed. The low temperature points are limited by thermal effects due to the low quality factor at high fields, shown in Fig 11. The thermometry is on the outer cavity wall, and so may be different from the temperature on the RF surface if there is significant heating due to the surface fields.

path due to scattering sites in the RF layer, but in principle other effects could also change κ of the material. Specific to this case, the 120°C bake appears to make Nb more strongly Type-II and thereby reduce H_{sh}. This leads naturally to ask if an alternative to the 120°C bake that eliminates high field Q-slope while not reducing the material's mean free path can be developed.

Though theoretical predictions with the Eilenberger equations are progressing, there is still a significant effort that needs to be done before they converge for low temperatures. Thus, the work here provides much needed measurements to help guide the further development of theory.

Finally, the question of whether these results can be reproduced for alternative materials such as Nb_3Sn or MgB_2 is of central importance. Work is progressing rapidly on the production of Nb_3Sn,[21] a material whose superheating field was never successfully measured and study of these materials are expected in the next year.

REFERENCES

[1] A. J. Dolgert, S. John Di Bartolo, and Alan T. Dorsey. Superheating Fields of Superconductors: Asymptotic Analysis and Numerical Results. *arXiv:cond-mat*, 1995.

[2] G. Catelani and James P. Sethna. Temperature dependence of the superheating field for superconductors in the high-κ London limit. *Physical Review B*, 78, 2008.

[3] R. Doll and P. Graf. Superheating in cylinders of pure superconducting tin. *Phys. Rev. Lett.*, 19(16):897–899, Oct 1967.

[4] A. B. Pippard. An experimental and theoretical study of the relation between magnetic field and current in a superconductor. *Proceedings of R. Soc. London Ser. A*, 216, 1991.

[5] Merrill, J. R. 1968, "Type II Superconductivity Experiment," American Journal of Physics, 36, 133.

[6] Matricon, J. and Saint-James, D. "Superheating Fields in Superconductors," 1967, Physics Letters A, 24, 241.

[7] L. P. Gor'kov and G. M. Eliashberg. Generalization of the Ginzburg-Landau Equations for Non-stationary Problems in the Case of Alloys with Paramagnetic Impurities. *Soviet Journal of Experimental and Theoretical Physics*, 27:328–+, August 1968.

[8] G. Eilenberger. *Z. Phys.*, 214, 1968.

[9] D. K. Finnemore, T. F. Stromberg, and C. A. Swenson. Superconducting properties of high-purity niobium. *Phys. Rev.*, 149(1):231–243, Sep 1966.

[10] J.C. Renard and Y.A. Rocher. Superheating in pure superconducting niobium. *Physics Letters A*, 24(10):509 – 511, 1967.

[11] T. Yogi, G. J. Dick, and J. E. Mercereau. Critical rf magnetic fields for some type-i and type-ii superconductors. *Phys. Rev. Lett.*, 39(13):826–829, Sep 1977.

[12] I. E. Campisi and Z. D. Farkas. High-Gradient, Pulsed Operation of Superconducting Niobium Cavities. *SLAC AP-16*, 1984.

[13] Z. D. Farkas. Low Loss Pulsed Mode Cavity Behavior. *SLAC AP-15*, 1984.

[14] T. Hays, H. S. Padamsee, and R. W. Roth. Response of superconducting cavities to high peak power. In *Proceedings of the 1995 U.S. Particle Accelerator Conference*, 1995.

[15] J. Sethna and M. Transtrum. Personal Communication, 2009.

[16] T. Hays and H. S. Padamsee. Determining H_c^{RF} for Nb and Nb_3Sn through HPP and Transient Q Analysis. In *7th Workshop on RF Superconductivity*, 1995.

[17] H. Padamsee, J. Knobloch, and T. Hays. *RF Superconductivity for Accelerators*. Wiley, 1998.

[18] G. Eremeev and H. S. Padamsee. Change in High Field Q-Slope by Baking and Anodizing. *Physica C: Superconductivity*, 2006.

[19] J. Halbritter, "Fortran-program for the computation of the surface impedance of superconductors," KAROLA - OA-Volltextserver des Forschungszentrums Karlsruhe [http://opac.fzk.de:81/oai/oai-2.0.cmp.S] (Germany), 1970.

[20] G. Ciovati, "Effect of low-temperature baking on the radio-frequency properties of niobium superconducting cavities for particle accelerators," Journal of Applied Physics, 96, 2004.

[21] S. Posen and M. Liepe. "Stochiometric Nb_3Sn in first samples coated at Cornell," Proceedings of the 15th International Conference on RF Superconductivity, 2011.